Dynamics of the plasma plume
induced during laser welding

Tomasz Mościcki, Jacek Hoffman, Zygmunt Szymański

Institute of Fundamental Technological Research, ul. Świętokrzyska 21, 00–049 Warszawa, Poland,
e-mail: tmosc@ippt.gov.pl.

The dynamics of the plasma plume produced during laser welding is quite complex. The keyhole
wall oscillates and this results in oscillations of the plasma plume over the keyhole mouth. The
metal vapour, which appears in irregular bursts, interacts with the shielding gas flowing from the
opposite direction. In the present work, temporary electron densities and temperatures are
determined in the peaks of plasma bursts during welding with a continuous wave CO_2 laser. It has
been found that during strong bursts the plasma plume over the keyhole consists of metal vapour
only, without being diluted by the shielding gas. The results, together with the analysis of the
colour pictures from streak camera, allow interpretation of the dynamics of the plasma plume. No
apparent mixing of metal vapour and the shielding gas has been observed. In typical bursts the
electron density determined from the Stark broadening of Ar I lines varies from 0.9×10^{23} m^{-3} near
the metal surface to 0.5×10^{23} m^{-3} at a distance of 1.5 mm from the surface. Assuming that argon
is not mixed with the metal vapour and is in local thermal equilibrium these electron densities
correspond to temperatures 12.7 kK and 11.5 kK, respectively. In strong bursts the electron density
varies, along the same distance, from 1.6×10^{23} m^{-3} to 0.6×10^{23} m^{-3}, which corresponds to the
temperatures of 14.2 kK and 11.8 kK, respectively.

Keywords: laser welding, plasma diagnostics.

1. Introduction

The composition of the plasma plume induced during laser welding has remarkable
effect on the absorption and refraction of CO_2 laser radiation. It is usually assumed
that the plasma plume consists of ionized metal vapour diluted with the shielding
gas [1], [2]. In paper [1], the composition of the metal vapour-argon mixture was
calculated from the ratios of intensities of Ar I lines and the metal lines, emitted from
the same plasma region. Since the measurements were neither space- nor time resolved
the measured intensities represented certain space- and time-averaged values
integrated over the plasma depth and the detector runtime. The calculations were made
assuming that the plume is the mixture of the metal vapour and argon in local
thermodynamic equilibrium (LTE). The total plasma pressure of 0.1 MPa

(atmospheric) was assumed, with the average temperature of 11000 K and the electron density equal to 1.1×10^{23} m^{-3}.

The average partial pressure of the metal vapour $p_i + p_a$ was found to be about 0.02 MPa, the argon partial pressure ~0.06 MPa, and the remaining pressure was due to electrons in both cases of Fe-Ar and Ti-Ar plasmas [1]. The main contribution to the metal-vapour pressure was due to the ions; the atomic metal-vapour density was about one order of magnitude lower. Argon was weakly ionized and most of the electrons stemmed from the ionized metal vapour, provided that the average plasma temperature did not exceed 12000 K.

Such a composition of the plasma plume is consistent with electron densities determined from the Stark broadening of the 5383.37 Å Fe I line. It has been found numerically that the electron densities and temperatures determined from the Fe I lines correspond to regions at a temperature of ~ 8700 K or lower [1], even if plasma temperature is higher. Calculations show that in the pure iron plasma at a temperature of 8700 K, the electron density is equal to $\sim 2 \times 10^{23}$ m^{-3}. Although the maximum electron temperature determined experimentally from the Fe I lines is about 8700 K, the electron density determined from the broadening of the 5383.37 Å Fe I line does not exceed 8.5×10^{22} m^{-3}. The difference between the experimental and calculated electron densities is therefore significant, much larger than the estimated experimental error. The measured N_e value fits then better to the Fe-Ar composition of the plasma plume and has been taken as supplementary evidence for mixing of both gases.

However, the mixing region of both gases, the metal vapour and the shielding gas, is not well known yet. It is not clear whether the mixing takes place only in a limited area close to the interface between two gases or whether it extends deeper in the keyhole. Although the measurements allow the vertical resolution of the plasma, its radial distribution is not known. Due to plasma instabilities [3] the Abel inversion leads to large errors and therefore it is not performed.

In the present paper, we propose the explanation of plasma plume dynamics based on the time-resolved measurements of the spectral lines of argon and metal as well as on the interpretation of colour plasma pictures taken with a streak camera [3]. The calculations of the emission coefficients of the iron and argon plasma in the visible region together with the colour analysis allow us to distinguish between argon and metal plasma.

The problem is interesting because of the growing need for a reliable method of on-line process monitoring. Most of the methods are based on optical signals from the plasma. It is obvious that better understanding of the plasma dynamics can lead to better monitoring of the process.

2. Time-resolved spectral measurements

Conditions of the experiment were as follows [4]. Welding was done with the continuous wave CO_2 laser, Photon Sources VFA 2500, operating at the power of ~1.75 kW. Argon was used as a shielding gas. The welded metal was stainless steel,

2 mm thick, containing 2.0% Mn, 0.8% Si, 17% Cr, 10% Ni, and remainder Fe. Welding speed was 1 m/min. The experimental setup for registration of the emission spectra consisted of a 1.3 m focal length spectrograph, image intensifier and a 1254 silicon intensified target (SIT) detector connected to optical multichannel analyzer (OMA). Fast gate image intensifier coupled to the detector amplified light signal and allowed fast, time-resolved photodetection. The spectra below 5900 Å were taken on the second order of diffraction where the reciprocal dispersion of the spectrograph was 3 Å/mm. The image intensifier was gated for 2 μs by a high voltage (HV) pulse generator triggered by the signal from a comparator. As a reference, the signal from a photodiode measuring the broadband radiation from the plasma plume was used. The HV pulser was triggered when the signal from the photodiode exceeded certain level. The same signal triggered the OMA controller and started data acquisition. Optical signal from plasma was sent to the photodiode with fibre optics. The signal from the photodiode was registered on the oscilloscope and the triggering level was adjusted so as to collect spectra during selected moments of plasma oscillations.

The signal from the photodiode, as presented in Fig. 1, shows that the plasma appears in more or less regular pulses. A series of bursts of similar amplitude is usually followed by a much larger pulse. Therefore, two triggering levels were used, low and high. The low level was adjusted so as to collect spectra during the peak of typical amplitude, whereas the high level was used to collect spectra during strong plasma bursts.

The entrance slit of the spectrograph was perpendicular to the metal surface so the successive tracks of the detector recorded radiation from the plasma slices situated at different distances (heights) from the metal surface. The measured line intensities are integrated over the plasma depth seen by the detector. The apparatus half-width
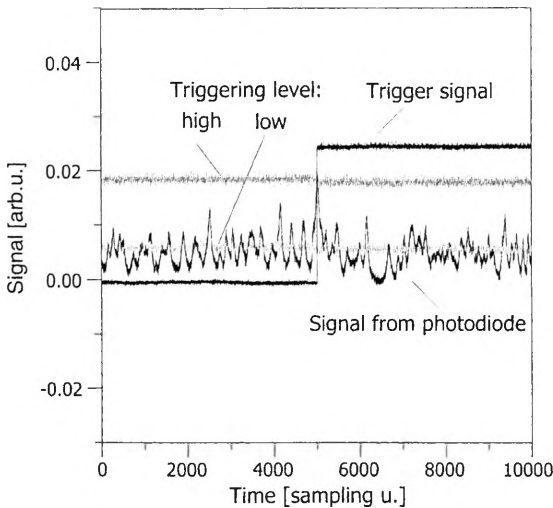

Fig. 1. Signal from photodiode, triggering level and trigger signal initiating high voltage pulse. Sampling unit 1 μs.

(FWHM) was measured with the use of a He-Ne laser to be about 0.2 Å (on the second order of diffraction) and the Doppler half-width did not exceed 0.05 Å. The typical spectra collected in the peaks of typical and strong plasma pulses are shown in Fig. 2a and b, respectively. In the figures only single tracks near the metal surface are presented but the ratios of intensities of Ar and Fe lines do not change significantly with the distance from the surface.
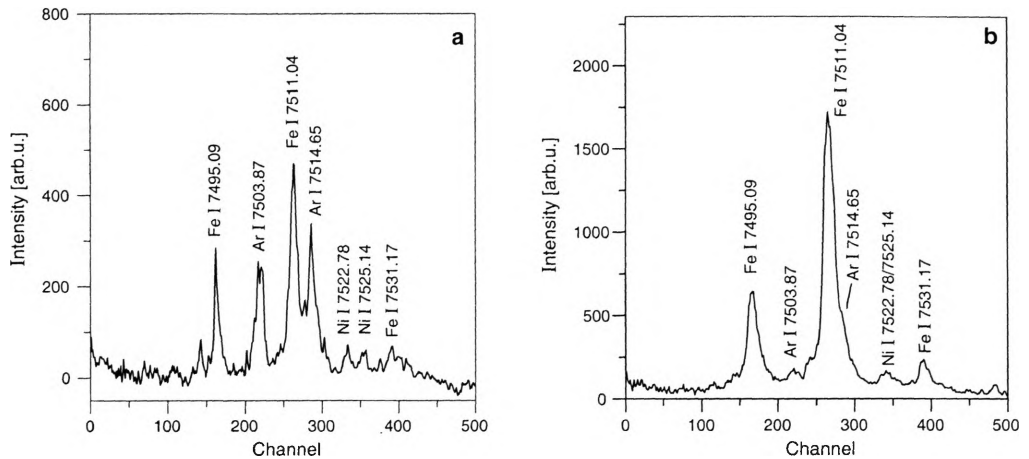

Fig. 2. Iron and argon lines registered in typical (a) and strong (b) plasma burst. Single track near the metal surface. Negative intensities at some wavelengths in figure a are artificial and result from the subtraction of the electronic background.

The results show that the composition of the plasma plume is not constant. During typical pulses the argon spectral lines are always present and they often are more intense than the iron lines. During strong plasma bursts argon is hardly seen – plasma plume consists mainly of the metal vapour. Sometimes argon lines during strong plasma bursts are present and then the electron density can be determined from Stark broadening of Ar I 7503.87 and 7514.65 Å lines [1]. Peak electron densities reach 1.6×10^{23} m^{-3}, which is 30% higher than the time-averaged value. The results will be examined after the analysis of colour photographs of the plasma plume.

3. Plasma visible radiation

The spectroscopic measurements give no information about the distribution of the shielding gas and metal vapour in the plume. Some additional information can be drawn from the colour pictures of the plasma plume taken with the streak camera [3]. The calculations of the emission coefficients of the iron and argon plasmas in the visible region together with the colour analysis allow us to distinguish between argon and metal plasma.

Plasma plume radiation was calculated as the sum of the line emission coefficients [5]

$$\varepsilon = \frac{1}{4\pi} \sum_{z=1}^{3} \sum_{k} A_{ki} \frac{hc}{\lambda_{ki}} g_k \frac{n_z}{U_z} \exp\left(-\frac{E_{z,k}}{kT}\right) \qquad (1)$$

where n_z, g_k, and $E_{z,k}$ are particle density, statistical weight, and excitation energy of level k, respectively, $U_z(T)$ – the partition function of particles with the charge z, A_{ki} – the transition probability, λ_{ki} – the wavelength of the spectral line, h – the Planck constant, and c – the light velocity. Calculations were made for argon and iron in the extended visible region 3800–7500 Å necessary to evaluate the colour. Plasma composition was calculated at a pressure of 0.1 MPa assuming local thermal equilibrium. In the case of argon 518 spectral lines were taken into account, 320 of Ar I, 190 of Ar II and 8 of Ar III. In the case of iron 1925 spectral lines were used, 1546 of Fe I, 259 of Fe II and 120 of Fe III. The transition probabilities, excitation energies and statistical weights were taken from the NIST Atomic Database [6]. The partition functions were taken from [7], [8]. Continuous emission coefficients due to bremsstrahlung and recombination radiation did not exceed a few percent of total radiation and have been neglected. Under conditions of our experiment argon lines are free from self-absorption. Self-absorption of iron lines was not taken into account either. Alghough simulations shows that absorption cannot be totally neglected its influence on the colour is negligible. In view of uncertainty of plasma temperature and composition (partial pressure of components) detailed computation of self-absorption has not been made.

Total emission coefficients of iron and argon lines in the region of 3800–7500 Å at the temperature of 10000 K are shown in Fig. 3. Their dependence on wavelength
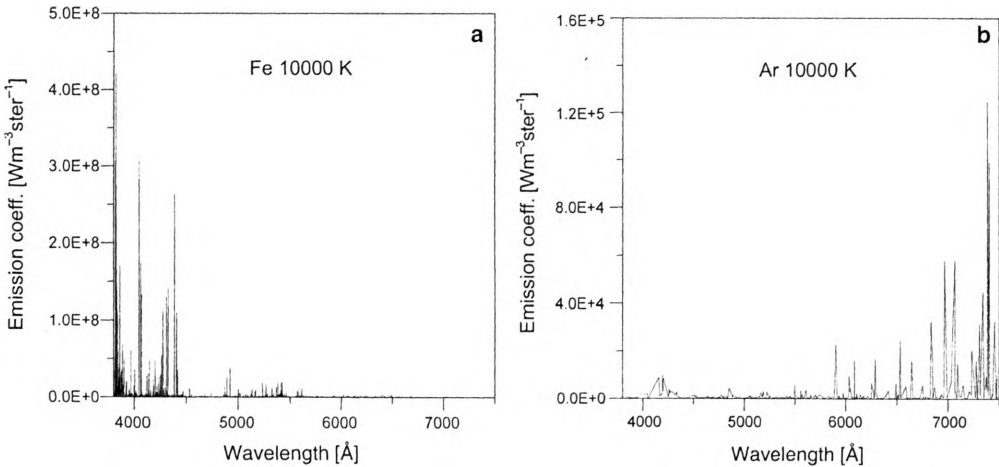

Fig. 3. Emission coefficient of iron (**a**) and argon (**b**) lines in the range of 3800–7500 Å at the temperature of 10000 K.

is very different, which allows identification of both components, argon and metal vapour, in the plasma plume.

Figure 4 shows the radiation power of iron and argon in the visible range in terms of the plasma temperature. It is clear that iron plasma radiates much more energy than argon. Even at a temperature of 15 kK argon radiation amounts merely to 10% of the iron radiation. At a temperature of 10 kK one cubic mm (approximate dimension of the plume) of the iron plasma radiates about 50 watts in a full solid angle.
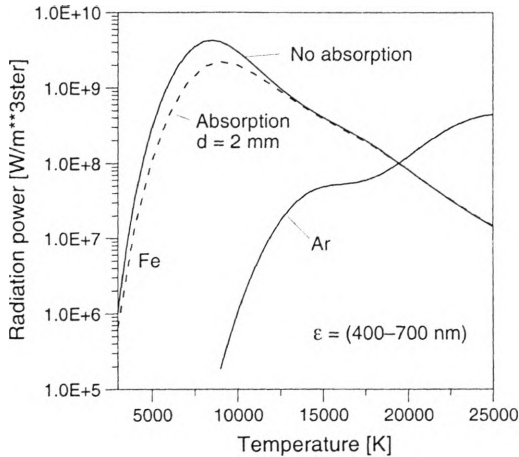

Fig. 4. Radiation power of iron and argon lines in the visible region *vs.* temperature. Broken line shows effect of self-absorption for isothermal iron plasma sphere with diameter of 2 mm.

The results obtained from the NIST data have been compared with the results obtained with the use of theoretically calculated iron transition probabilities [9]. The agreement with the experimental data is very good. For example, the total radiation power is only 20–25% higher than that obtained from the NIST data, which is obvious given that, contrary to the NIST data, the theoretical data include all transitions.

4. Colour analysis

Having calculated the emission coefficient one can determine the colour of light emitted by the plasma plume. The CIE colour-matching functions [10] used to specify the colour are shown in Fig. 5. The CIE primaries X, Y, Z needed to match a colour with a spectral energy distribution $P(\lambda)$, are:

$$X = k\int P(\lambda)\bar{x}_\lambda \mathrm{d}\lambda, \quad Y = k\int P(\lambda)\bar{y}_\lambda \mathrm{d}\lambda, \quad Z = k\int P(\lambda)\bar{z}_\lambda \mathrm{d}\lambda \tag{2}$$

where $k = 680$ lumens/watt for self-luminous objects and $\bar{x}, \bar{y}, \bar{z}$ denote colour matching function [9]. Chromaticity values are defined as [10]:
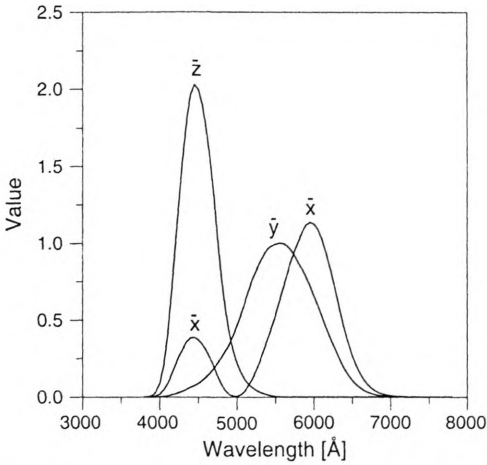
Fig. 5. Colour-matching functions for the CIE 1964.

$$x = \frac{X}{X + Y + Z}, \qquad y = \frac{Y}{X + Y + Z}, \qquad z = \frac{Z}{X + Y + Z}. \qquad (3)$$

Having specified x, y one can determine z by $z = 1 - x - y$.

The CIE diagram together with calculated colours of iron and argon plasma at various temperatures is shown in Fig. 6. The pure spectral light colours lie on the curved boundary of the diagram; they are fully saturated. Other colours are developed by mixing different wavelengths; their saturation is equal to the ratio of the dominant
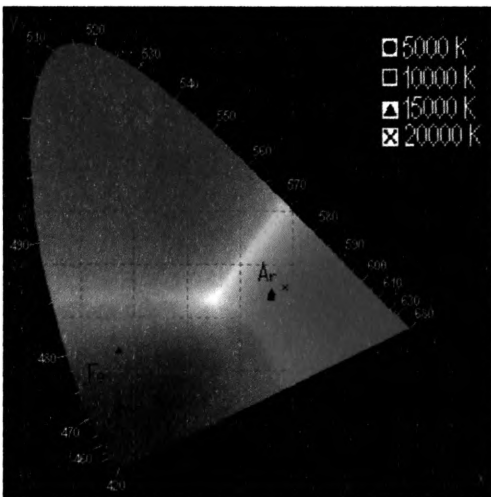

Fig. 6. CIE chromaticity diagram (reprinted with permission of efg's Computer Lab [11]) with calculated colours of iron and argon plasma at various temperatures.

wavelength to other wavelengths. In the case of white light contributions of all wavelengths are balanced.

The colour is light or dark in dependance on the luminance. The dependence on luminance is not shown in the diagram. With growing luminance all colours which are not pure become brighter and finally tend to being white. This fact is seen in the over -illuminated pictures. At low luminance all desaturated colours become darker and tend to black with zero luminance.

5. Dynamics of plasma plume

The calculations of plasma emission coefficients together with analysis of plasma colour (CIE analysis) show that the iron plasma is blue while the argon plasma is pinkish. Although, in the present paper, there is no room for full analysis of the plasma plume dynamics, from the colour photographs made with the streak camera some characteristic patterns of the plasma plume can be distinguished.

The first photograph shown in the first row of Fig. 7 shows the pinkish egg-like argon plasma, situated in the centre over the keyhole mouth. The bluish metal plasma emerges from the keyhole and flows around at each side of the argon plasma. The flow rate of the metal vapour decreases and metal plasma gradually extinguishes. The second row represents the burst of bluish metal vapour plasma streaming from the keyhole. The argon plasma disappears and develops again. The last two exposures of the second row show another burst of the metal plasma. This time bluish metal vapour plasma streams to the right from behind the argon plasma. The third row shows a new burst of metal plasma.
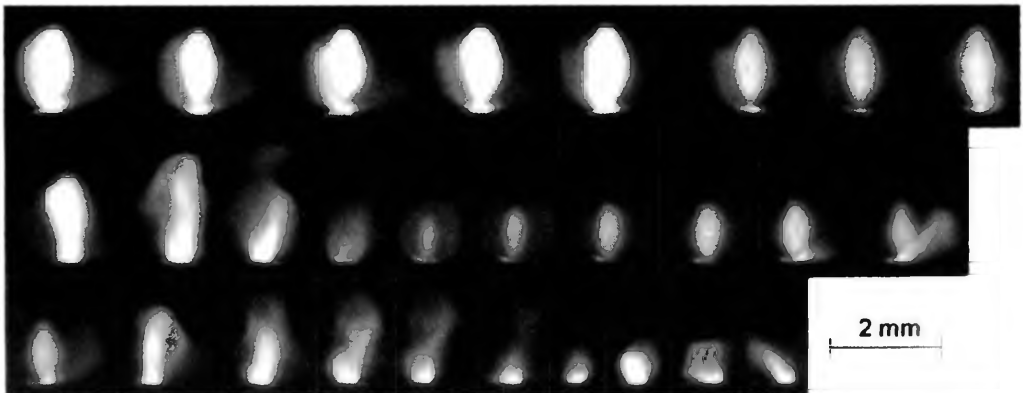

Fig. 7. Plasma plume pictures taken with a streak camera (after [3]). Exposure time 10 μs, frame interval 40 μs. Laser power 2 kW. Welded material stainless steel 2 mm thick. Welding speed 1 m/min. Shielding gas argon 10 l/min. Maximum height of the plume ~2 mm. Bluish plume – metal vapour plasma, pinkish plume – argon plasma.

No apparent mixing of the two gases is observed, although the presence of argon in the iron plasma cannot be excluded; even partial pressure of argon ~0.06 MPa does not change the hue significantly – plasma remains bluish.

As the exposure time is only 10 μs, only dense, hot plasma core is seen in the pictures; cooler plasma boundary extends actually farther. Sometimes the argon plasma is not seen but this does not mean that it is absent. The jet of metallic plasma changes direction and once in a while it may screen off the argon plasma from the camera. When helium is used as a shielding gas such pictures are not observed because high ionisation potential of helium prevents its ionisation.

The three patterns described above are depicted schematically in Fig. 8a, b, c.
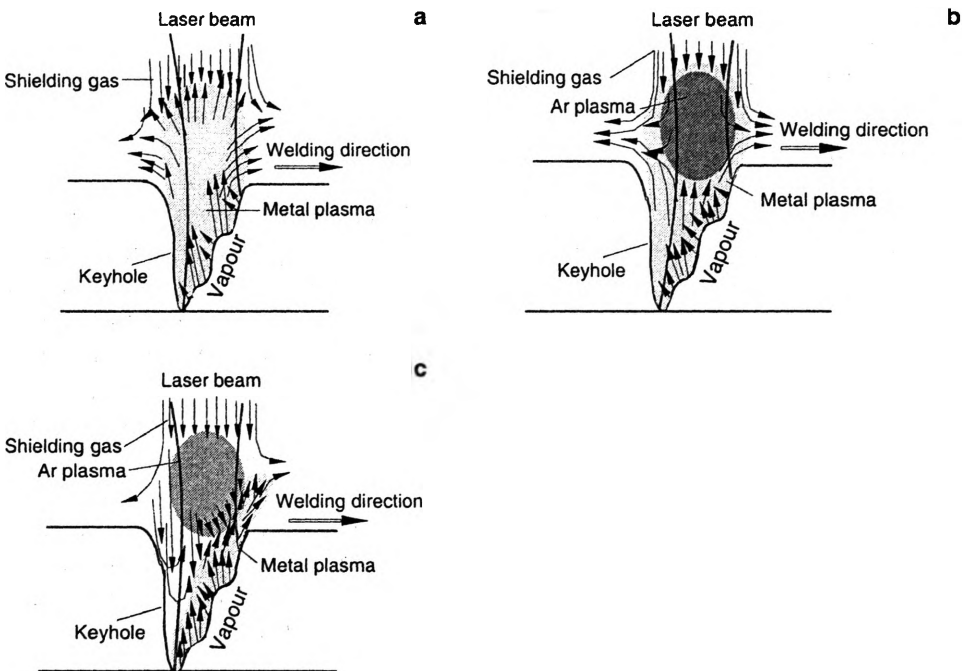

Fig. 8. Possible shielding gas-metal vapour interaction: burst of the metal plasma (**a**), metal plasma flows around at each side of the argon plasma (**b**), metal plasma streams from one side of the keyhole mouth (**c**).

With an increase of the argon flow rate the plasma plume dimension decreases due to better cooling but the plasma plume pictures show essentially the same patterns. In the case of helium plasma the patterns are less complex because helium is not ionized and does not form such an obstacle for metal vapour as the hot argon plasma. When the flow penetrates a region of increasing temperature, its behaviour is similar to a flow past an obstacle. Most of the stream lines bypass the plasma region – only a relatively small part of them enter the hot region [12].

Let us go back to the spectroscopic measurements. In typical bursts the space-averaged electron density determined from the Stark broadening of Ar I lines varies from 0.9×10^{23} m^{-3} near the metal surface to 0.5×10^{23} m^{-3} at a distance of 1.5 mm from the surface. Assuming that argon is not mixed with the metal vapour and is in local thermal equilibrium these electron densities correspond to temperatures 12.7 kK and 11.5 kK, respectively. In strong bursts the electron densities vary, along the same distance, from 1.6×10^{23} m^{-3} to 0.6×10^{23} m^{-3}, which correspond to temperatures 14.2 kK and 11.8 kK, respectively.

The space-averaged electron densities determined from the Stark broadening of Fe I 5383.37 Å line are about 25–30% lower than those obtained from the argon lines. In the case of pure iron plasma their maximum values corresponded to the temperature of about 7500 K. This result is somewhat confusing because the temperature measurements [1] suggest rather higher values of the temperature and hence the electron density in the case of pure iron plasma.

6. Conclusions

The time-resolved spectroscopic measurements indicate that the iron lines are always present but the intensity of argon lines changes from strong to very weak. This is consistent with the colour pictures taken by streak camera showing the presence of the argon plasma only during weak vapour bursts. During the strong bursts the plasma plume over the keyhole consists of pure metal vapour not diluted by the shielding gas.

The dynamics of the plasma plume is quite complex. At least three major patterns are observed in the colour pictures of plasma plume taken with a streak camera; strong bursts of metal vapour with no argon plasma, bursts of the metal vapour streaming either around the argon plasma centered over the keyhole mouth or at one side of it.

No mixing of two gases is observed, although the admixture of argon in the iron plasma cannot be excluded. This is in agreement with the numerical simulation. Opposed jets with Reynolds number $Re \approx 200$ [13] similar to our case, show no mixing in a time scale characteristic of the plasma bursts during the laser welding.

References

[1] Szymański Z., Kurzyna J., Kalita W., J. Phys. D: Appl. Phys. **30** (1997), 3153.

[2] Beck M., Berger P., Huegel H., J. Phys. D: Appl. Phys. **28** (1995), 2430 .

[3] Kurzyna J., Szymański Z., Peradzyński Z., J. Tech. Phys. **36** (1995), 131.

[4] Hoffman J., Szymański Z., Czech. J. Physics, Suppl. D **52** (2002), D272.

[5] Lochte-Holtgreven W., Richter J., [In] *Plasma Diagnostics*, [Ed.] W. Lochte-Holtgreven, North Holland Pub. Co., Amsterdam 1968.

[6] NIST Atomic Spectroscopic Database: http://physics.nist.gov/PhysRefData/contents.html.

[7] HALENKA J., GRABOWSKI B., Astron. Astrophys. Suppl. Ser. **57** (1984), 43.

[8] DRAWIN H-W., FELENBOK P., *Data for Plasmas in Local Thermodynamic Equilibrium*, Gauthier -Villars, Paris 1965

[9] NAHAR N.S., Astron. Astrophys. **293** (1995), 967.

[10] FOLEY J.D., VAN DAM A., FEINER S.K., HUGHES J.F., *Computer Graphics, Principles and Practice*, Addison-Wesley Publishing Company, Reading, Massachusetts 1996.

[11] GLYNN II E.F., http://www.efg2.com/Lab/Graphics/Colors/Chromaticity.htm.

[12] SZYMAŃSKI Z., Arch. Mech. **50** (1998), 207.

[13] NAKAMURA S., BRODKEY R.S., Proceedings of the ASME Fluids Engineering Summer Conference, Boston, Massachusetts, 2000; http://olen.eng.ohio-state.edu/papers/11007.PDF.